Temperature dependence of the concentration fluctuation, the Kirkwood-Buff parameters, and the correlation length of tert-butyl alcohol and water mixtures studied by small-angle X-...

ARTICLE *in* THE JOURNAL OF PHYSICAL CHEMISTRY · AUGUST 1989

DOI: 10.1021/j100354a054

3 AUTHORS, INCLUDING:

Keiko Nishikawa
Chiba University
217 PUBLICATIONS **3,957** CITATIONS
SEE PROFILE

Hisashi Hayashi
Japan Women's University
83 PUBLICATIONS **872** CITATIONS
SEE PROFILE

spacing and orientation of the chains. It should be pointed out here that the difference between bulk hydrocarbon and apparent core densities can be explained by two reasons: (a) the two phases are different in the number of terminal hydrogen atoms per alkyl chain, and (b) the molar volume of the terminal hydrogen atom in micelles is significantly less than that in the bulk.

Finally, an attempt is made for guessing the number of solvent molecules penetrated in the micellar core. The total volume occupied by solvent molecules is $\Delta\Phi(H_2O) = V^*(H) - \Phi_a(H)$. By definition, the molar volume of solvent molecules inside the micelles is the same as in the bulk; thus, $w = \Delta\Phi(H_2O)/V_w^*$, resulting in $w \approx 0.45$. This result is in good agreement with the upper limit obtained from SANS;[2] the agreement of results originating from totally different considerations and experimental methods suggests that the present approach to w may not be entirely arbitrary.

Registry No. D, 7782-39-0; NaDS, 142-87-0; NaDDS, 151-21-3; NaTDS, 1191-50-0.

Supplementary Material Available: Table containing raw sodium alkyl sulfate density and apparent molar volume data in normal and 99.85% heavy water vs surfactant aquamolality (2 pages). Ordering information is given on any current masthead page.

Temperature Dependence of the Concentration Fluctuation, the Kirkwood–Buff Parameters, and the Correlation Length of *tert*-Butyl Alcohol and Water Mixtures Studied by Small-Angle X-ray Scattering

Keiko Nishikawa,* Hisashi Hayashi, and Takao Iijima

Department of Chemistry, Faculty of Science, Gakushuin University, Mejiro, Toshima-ku, Tokyo 171, Japan
(Received: February 9, 1989; In Final Form: April 24, 1989)

Small-angle X-ray scattering measurements have been carried out on *tert*-butyl alcohol (TBA)–water mixtures at 28, 40, and 55 °C. The temperature effects in the concentration fluctuation and the Kirkwood–Buff parameters have been studied. Debye's correlation length has also been determined for each temperature. With the increase of temperature, the fluctuation becomes larger and the correlation length becomes longer, which indicates that the microscopic demixing of the mixture proceeds as the temperature is raised. The temperature and concentration dependences of the mixing state of the TBA–water solution are discussed.

Introduction

tert-Butyl alcohol (TBA) is miscible with water in all proportions and at any temperature of the liquid state in spite of having a fairly large hydrophobic group. However, TBA–water mixtures exhibit many anomalous physical properties, which have attracted much attention. In a previous paper, the concentration fluctuation and the Kirkwood–Buff parameters for TBA–water mixtures obtained by the small-angle X-ray scattering (SAXS) at 20 °C were reported.[1] The SAXS results were consistent with the light scattering data in the small concentration range.[2,3]

For temperatures 17.5–63 °C, Iwasaki and Fujiyama reported the light scattering measurements of TBA–water mixtures.[3] In the present work, the SAXS intensities from the mixtures of the concentration c_1 = 0–0.30 (c_1 = mole fraction of TBA) have been measured at 28, 40, and 55 °C, for the purpose of providing data in the concentration range where light scattering data are not available, and the temperature effects in the concentration fluctuation and the Kirkwood–Buff parameters have been observed.

Debye's correlation lengths were determined from the scattering curves. By dynamic light scattering using photon correlation spectroscopy,[4] Euliss and Sorensen[5] and Bender and Pecora[6] observed the correlation length ξ of the TBA–water mixtures for the temperatures 10–45 °C. Since their correlation length is probably a representation of the size of moving units, it is interesting to compare it with Debye's correlation length from SAXS, which is a measure of radii of clusterlike aggregates in the statistical configuration of the mixtures viewed over a long time. On the basis of the concentration fluctuation and the Kirkwood–Buff parameters as well as the correlation lengths, the temperature and concentration dependences of the mixing state of the TBA–water solution are discussed.

Experimental Section

Apparatus. A constructed apparatus with a focusing bent mirror was used for the measurement. The apparatus is the same as was reported in the previous paper,[1] except that a sealed-off tube with a Cu target was used in the present work instead of rotating anode tube. The X-rays from a sealed-off tube are of course weaker. However, a sealed-off tube with an appropriate safety system has an advantage: it can be operated in an "unmanned" mode. The s region ($s = (4\pi/\lambda)\sin\theta$, where 2θ = scattering angle and λ = X-ray wavelength) ranging from 0.05 to 0.7 Å^{-1} can be covered by this optical system.

Measurements. The scattering intensities from the solutions of 0.04, 0.05, 0.07, 0.10, 0.14, 0.17, 0.20, and 0.30 mole fraction of TBA were measured at the temperatures 28, 40, and 55 °C. In the present paper, the concentration of the solution is given in terms of the mole fraction of TBA denoted by c_1. The sample was enclosed in a holder with Mylar windows with a thickness of 25 μm. The thickness of the sample is ca. 1.50 mm. The temperature of the sample was controlled by heating with a sheathed heater and was monitored by a copper–constantan thermocouple. The constancy of the temperature was ±0.5 °C. The scattering intensities from pure water and background intensities from an empty sample holder were also measured as well as those from the solutions. The scattering intensity from pure water was used to calibrate the intensities to an absolute scale. The accumulating times for samples were 30 000–80 000 s.

The data have been corrected for the background intensities and the effects of slit height, multiple scattering, and absorption.[1] An absolute scale of the scattering intensities from the solution

(1) Nishikawa, K.; Kodera, Y.; Iijima, T. *J. Phys. Chem.* **1987**, *91*, 3694.
(2) Iwasaki, K.; Fujiyama, T. *J. Phys. Chem.* **1977**, *81*, 1908.
(3) Iwasaki, K.; Fujiyama, T. *J. Phys. Chem.* **1979**, *83*, 463.
(4) Berne, B.; Pecora, R. *Dynamic Light Scattering*; Wiley: New York, 1976.
(5) Euliss, G. W.; Sorensen, C. M. *J. Chem. Phys.* **1984**, *80*, 4767.
(6) Bender, T. M.; Pecora, R. *J. Phys. Chem.* **1986**, *90*, 1700.

0022-3654/89/2093-6559$01.50/0

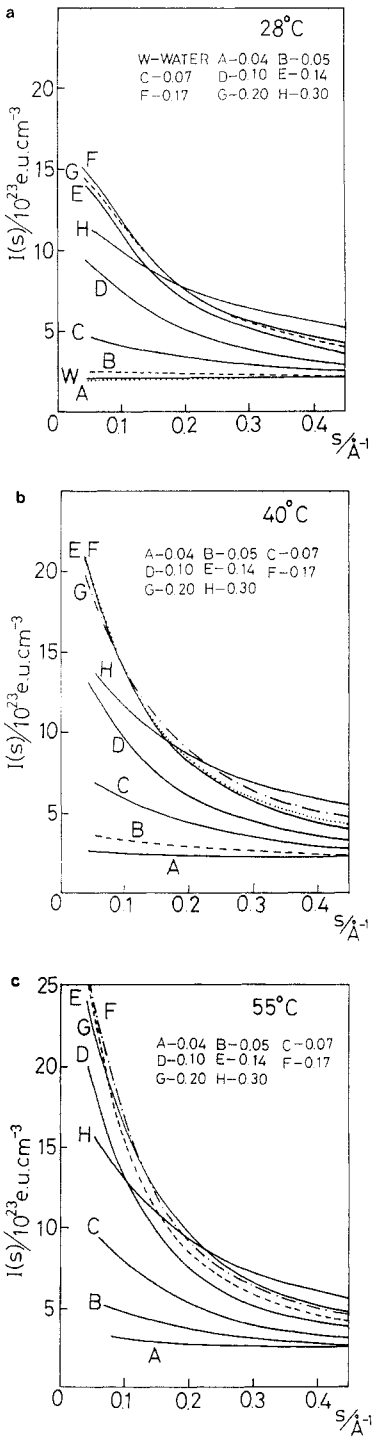

Figure 1. Small-angle X-ray scattering intensities in electron units per 1 cm³ against the scattering parameter s at 28 °C (a), 40 °C (b), and 55 °C (c).

was obtained by comparing the experimental intensity of pure water scaled by the theoretical value given by

$$I(0) = Z_w^2 N^2 \kappa^w_T kT/V \quad (1)$$

where κ^w_T is the isothermal compressibility of water, Z_w is the number of electrons in a water molecule, N is the number of water molecules in the volume V, k is the Boltzmann constant, and T is the absolute temperature.

Results and Discussion

Zero-Angle X-ray Scattering Intensity. The scattering intensities of TBA–water solutions and pure water after several corrections are shown in Figure 1: a 28 °C; b 40 °C, and c 55 °C. They are intensities per 1 cm³ in absolute scale (electron units).

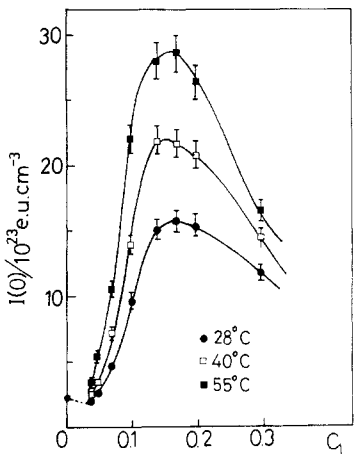

Figure 2. Temperature dependence of the zero-angle X-ray scattering intensities against the mole fraction of TBA (c_1).

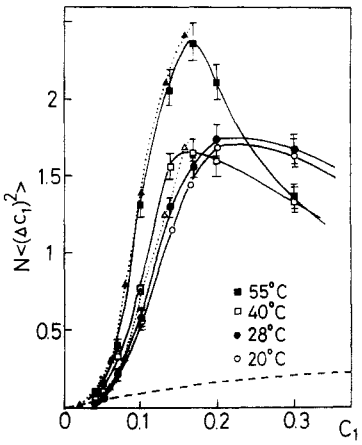

Figure 3. Concentration fluctuation of TBA–water mixtures at 20 °C (○), 28 °C (●), 40 °C (□), and 55 °C (■). The broken curve refers to the ideal solution. The dotted curves with triangles are the light scattering data by Iwasaki and Fujiyama at 24 °C (△) and 49.5 °C (▲).[3]

The zero-angle X-ray scattering intensities, $I(0)$, which were obtained by extrapolation of $s \rightarrow 0$, are shown in Figure 2, plotted against the mole fraction of TBA (c_1). Although a simple linear extrapolation to $s = 0$ was made in the previous work,[1] $I(0)$ has been determined by a curve fitting in the form of $I(s) = I(0) + bs^2 + cs^4$ in the present analysis because an intensity function tends to have a horizontal tangent as the s value approaches zero.

All the $I(0)$ vs c_1 curves have a notable maximum centered about $c_1 = 0.14$–0.17, which suggests large fluctuations in the concentration and the particle number. The second feature in the $I(0)$ curves is that the values become larger as the temperature increases. Thirdly, the $I(0)$ value at $c_1 = 0.04$ at 28 °C is less than that of pure water, which is the same feature as previously observed in the data at 20 °C.[1] However, at 40 and 55 °C, the $I(0)$ values at $c_1 = 0.04$ become larger than those of water. As was discussed in the previous paper,[1] the mixing state at $c_1 = 0.04$ is unique at room temperature.

Concentration Fluctuation. With zero-angle X-ray scattering intensities, $I(0)$, being utilized, in addition to the isothermal compressibility,[7,8] and the partial molar volume, the mean-square fluctuation in concentration $N\langle(\Delta c_1)^2\rangle$ and then the mean-square fluctuations in particle number $\langle(\Delta N)^2\rangle/N$ and their correlation $\langle(\Delta N)(\Delta c_1)\rangle$ have been obtained (the word "mean-square" is omitted hereafter). The partial molar volumes were calculated from the data of the apparent molar volumes by Visser et al.[9] The

(7) Nakagawa, M.; Inubushi, H.; Moriyoshi, T. *J. Chem. Thermodyn.* **1981**, *13*, 171.
(8) Kubota, H.; Tanaka, Y.; Makita, T. *Zairyo* **1984**, *33*, 107 (in Japanese).
(9) de Visser, C.; Perron, G.; Desnoyers, J. E. *Can. J. Chem.* **1977**, *55*, 856.

TABLE I: Zero-Angle Scattering, Fluctuations, and the Kirkwood-Buff Parameters of TBA (1)-Water (2) Solutions at 28, 40, and 55 °C

T/°C	c_1	$I(0)$/ 10^{23} eu cm^{-3}	$N\langle(\Delta c_1)^2\rangle$	$\langle(\Delta N)^2\rangle/N$	$\langle\Delta N\Delta c_1\rangle$	G_{11}/Å^3 molecule^{-1}	G_{22}/Å^3 molecule^{-1}	G_{12}/Å^3 molecule^{-1}
28	0.04	2.10	0.044	0.530	−0.146	−142	−5.4	−141
	0.05	2.61	0.080	0.898	−0.260	82	17	−202
	0.07	4.84	0.221	2.29	−0.704	489	113	−393
	0.10	9.88	0.620	5.52	−1.84	858	384	−735
	0.14	15.2	1.30	9.38	−3.48	869	837	−1029
	0.17	15.9	1.56	9.77	−3.89	598	1010	−972
	0.20	15.6	1.73	9.54	−4.06	393	1136	−887
	0.30	11.8	1.67	6.31	−3.23	−4	1159	−514
40	0.04	2.67	0.073	0.89	−0.25	320	15	−241
	0.05	3.57	0.126	1.47	−0.42	530	52	−329
	0.07	7.34	0.337	3.61	−1.10	1025	202	−613
	0.10	14.0	0.774	7.16	−2.34	1155	510	−931
	0.14	22.1	1.56	11.8	−4.28	1082	1058	−1249
	0.17	21.8	1.65	10.9	−4.23	615	1122	−1033
	0.20	20.9	1.60	9.50	−3.89	302	1100	−810
	0.30	14.5	1.33	5.49	−2.69	−65	953	−394
55	0.04	3.52	0.104	1.32	−0.36	813	40	−353
	0.05	5.54	0.204	2.47	−0.70	1296	113	−547
	0.07	10.6	0.472	5.20	−1.56	1652	310	−875
	0.10	22.1	1.31	12.1	−3.98	2278	908	−1601
	0.14	28.0	2.06	15.5	−5.63	1545	1424	−1663
	0.17	28.6	2.36	15.5	−6.03	1028	1643	−1499
	0.20	26.4	2.10	12.5	−5.11	486	1482	−1078
	0.30	16.6	1.37	5.80	−2.81	−69	1013	−404

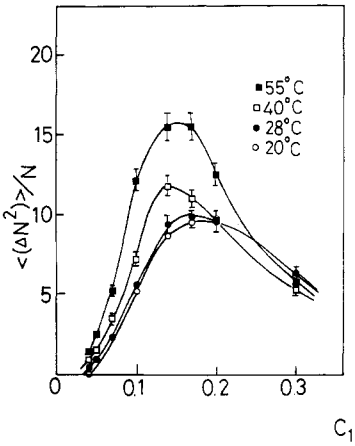

Figure 4. Temperature dependence of the fluctuation in the particle number of TBA–water mixtures.

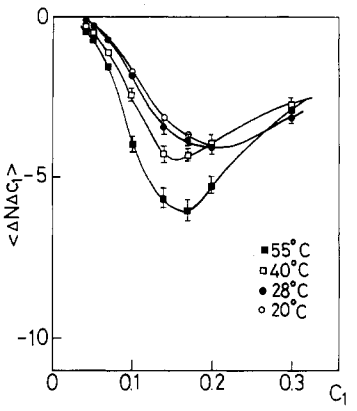

Figure 5. Temperature dependence of the correlation term of the fluctuations in the particle number and concentration.

method to obtain the fluctuations is given in ref 1, which is based on the theory by Bhatia and Thornton.[10] The values of the fluctuations are tabulated in Table I and shown in Figures 3–5, respectively, with the previous results at 20 °C.[1] The broken curves in Figure 3 refer to the ideal solutions, whose $N\langle(\Delta c_1)^2\rangle$ are given by $c_1(1 - c_1)$.[2] The curves for the fluctuations in the concentration and particle number have a maximum at $c_1 \simeq 0.2$ at the temperatures of 20 and 28 °C, and the maxima of the curves at 40 and 55 °C move toward lower concentration ($c_1 \simeq 0.17$). In the curves of the concentration fluctuation (Figure 3), the fluctuation becomes larger with the increase of the temperature up to $c_1 = 0.2$, while the lowering of the curves in c_1 regions larger than 0.2 is slower for lower temperatures and there are intersections of the curves.

Experimental errors of the concentration fluctuation were estimated in a way similar to that described in ref 1 and are shown by error bars in Figure 3.

The concentration fluctuation of the TBA–water mixtures obtained from the light scattering experiment was reported by Iwasaki and Fujiyama.[2,3] Their results for the temperatures at 24 and 49.5 °C are also shown in Figure 3. In their experiment, a laser beam with the wavelength of 6328 Å was used. Therefore, the s value in the light scattering experiment at a scattering angle of 90° corresponds to 0.002 Å^{-1}, which is much nearer to $s = 0$ than that of the present SAXS. By comparison, it is found that the values from the X-ray scattering experiment at 55 °C are in good agreement with the data at 49.5 °C by the light scattering technique, and our data at 28 °C agrees well with their result at 24 °C except only for the value at $c_1 = 0.15$. Though the comparison cannot be made in all the concentrations, the concentration fluctuation determined by the curve fitting extrapolation seems to be consistent with that by the light scattering experiment. It can be said that the difference in the wavelength does not affect the results for this system.

Kirkwood–Buff Parameters. The Kirkwood–Buff parameters[11] were obtained from the fluctuations.[1,12] The relation between the fluctuations and the Kirkwood–Buff parameters are given by eq 10 of ref 1. The Kirkwood–Buff parameters for TBA–water mixtures at 28, 40, and 55 °C are shown in Figure 6a–c with the results at 20 °C and tabulated in Table I. In the present paper, subscript 1 refers to TBA and subscript 2 refers to water.

The Kirkwood–Buff parameters, $G_{\alpha\beta}$, are defined by[11]

$$G_{\alpha\beta} = \int [g_{\alpha\beta}(r) - 1]4\pi r^2 \, dr \qquad (2)$$

where $g_{\alpha\beta}(r)$ is the partial distribution function. The Kirkwood–Buff parameters are a measure of the affinity of α molecules around a β molecule.[13] For the case of TBA molecules around

(10) Bhatia, A. B.; Thornton, D. E. *Phys. Rev. B* **1970**, *2*, 3004.

(11) Kirkwood, J. G.; Buff, F. P. *J. Chem. Phys.* **1951**, *19*, 774.
(12) Nishikawa, K. *Chem. Phys. Lett.* **1986**, *132*, 50.

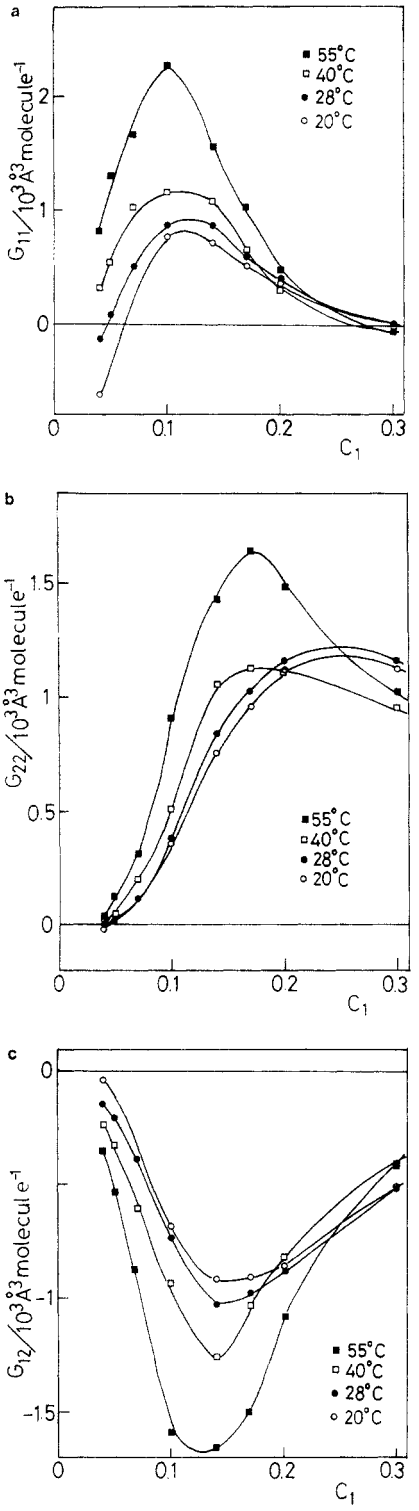

Figure 6. Temperature dependence of Kirkwood–Buff parameters of TBA–water mixtures: (a) G_{11}, (b) G_{22}, and (c) G_{12}.

a TBA molecule, namely G_{11} (Figure 6a), the curves have a maximum centered about $c_1 = 0.10$–0.12 and the maximum moves toward lower concentration with the increase of temperature. For the case of water molecules around a water molecule, G_{22} (Figure 6b), the center of the curves is about $c_1 = 0.17$–0.25 and the maximum moves also toward lower concentration as the temperature is raised. For the case of TBA molecules around a water molecule or water molecules around a TBA molecule, G_{12} (Figure 6c), the position of the minimum almost agrees with the maximum position of the concentration fluctuation.

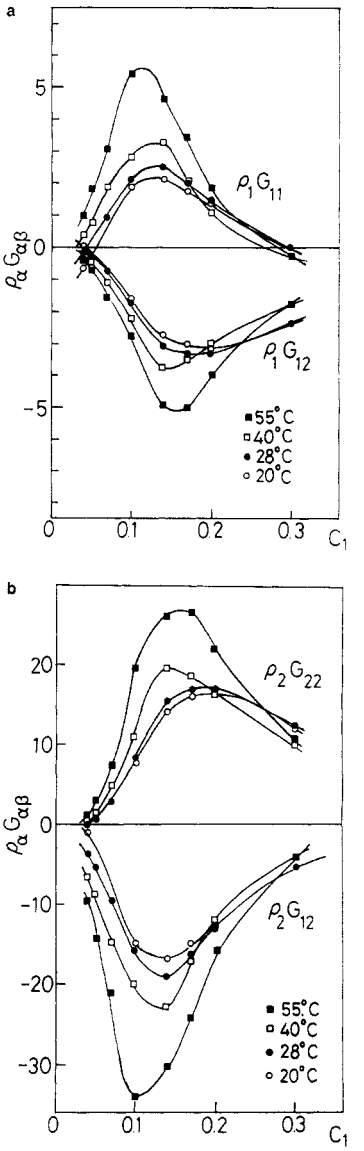

Figure 7. Temperature dependence of $\rho_\alpha G_{\alpha\beta}$ for TBA–water solutions.

The quantities $\rho_\alpha G_{\alpha\beta}$ are shown in Figure 7a,b. The physical meaning of $\rho_\alpha G_{\alpha\beta}$ is inferred from the definition of $G_{\alpha\beta}$[11] as follows:

$$\text{for } \alpha = \beta \qquad \rho_\alpha G_{\alpha\alpha} = \frac{\langle (\Delta N_\alpha)^2 \rangle}{\langle N_\alpha \rangle} - 1$$

$$\text{for } \alpha \neq \beta \qquad \rho_\alpha G_{\alpha\beta} = \frac{\langle \Delta N_\alpha \, \Delta N_\beta \rangle}{\langle N_\beta \rangle}$$

where N_α is the number of α particles in the volume concerned. Namely, the quantity $\rho_\alpha G_{\alpha\alpha} + 1$ is the mean-square fluctuation of the particle number of α molecules, and for $\alpha \neq \beta$, the quantity $\rho_\alpha G_{\alpha\beta}$ is the cross term of the fluctuation of N_α and N_β.

The absolute values of the Kirkwood–Buff parameters and $\rho_\alpha G_{\alpha\beta}$ also become larger as the temperature is raised, which suggests that the demixing of the mixtures proceeds with the increase of temperature.

Correlation Length. In addition to the fluctuations and Kirkwood–Buff parameters obtained from $I(0)$, we can determine the correlation length from the scattering curve. The X-ray total scattering intensity is expressed by the following relation[14]

$$I(s) = I_e \int \langle \Delta\rho_e(0) \, \Delta\rho_e(r) \rangle \frac{\sin(sr)}{sr} 4\pi r^2 \, dr \qquad (3)$$

where I_e is the scattering intensity of an electron and $\Delta\rho_e(r)$ is

(13) Ben-Naim, A. *J. Chem. Phys.* **1977**, *67*, 4884.

(14) Debye, P.; Bueche, A. M. *J. Appl. Phys.* **1949**, *20*, 518.

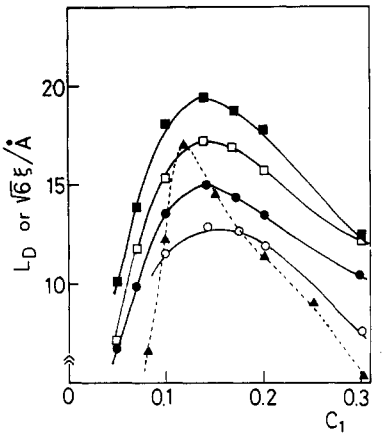

Figure 8. Debye's correlation length at 20 °C (○), 28 °C (●), 40 °C (□), and 55 °C (■). The dotted curve with triangles is from the data by Koga at 27 °C.[18]

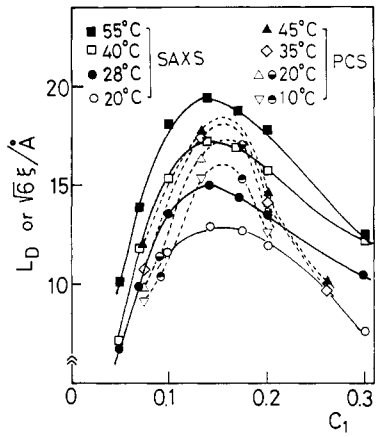

Figure 9. Comparison of the correlation lengths obtained by small-angle X-ray scattering (SAXS) [(○) 20 °C, (●) 28 °C, (□) 40 °C, and (■) 55 °C] and those by photon correlation spectroscopy (PCS) [(▽) 10 °C, (△) 20 °C, (◇) 35 °C, and (▲), 45 °C from ref 5 and (◒) 10 °C and (◒) 20 °C from ref 6).

the difference of the electron density from the average at the position r. Equation 3 is expanded as

$$I(s) = I_e \int \langle \Delta\rho_e(0)\ \Delta\rho_e(r)\rangle (1 - \tfrac{1}{6}r^2s^2 + \ldots) 4\pi r^2\, dr$$

$$I(s) \simeq I_e \int \langle \Delta\rho_e(0)\ \Delta\rho_e(r)\rangle 4\pi r^2\, dr \times \left[1 - \frac{\int r^2 \langle \Delta\rho_e(0)\ \Delta\rho_e(r)\rangle 4\pi r^2\, dr}{\int \langle \Delta\rho_e(0)\ \Delta\rho_e(r)\rangle 4\pi r^2\, dr} \frac{s^2}{6} + \ldots\right] = I_0\left(1 - \frac{s^2 L_D^2}{6} + \ldots\right) \quad (4)$$

where

$$I_0 = I_e \int \langle \Delta\rho_e(0)\ \Delta\rho_e(r)\rangle 4\pi r^2\, dr \quad (5)$$

and

$$L_D \equiv \left[\frac{\int r^2 \langle \Delta\rho_e(0)\ \Delta\rho_e(r)\rangle 4\pi r^2\, dr}{\int \langle \Delta\rho_e(0)\ \Delta\rho_e(r)\rangle 4\pi r^2\, dr}\right]^{1/2} \quad (6)$$

which is the correlation length or the persistence length defined by Debye.[15] The physical meaning of L_D^2 is the second moment of the correlation function for the fluctuation of the electron density. In Ornstein–Zernike theory, the scattering intensity near $s = 0$ is given by[16]

$$I(s) = \frac{I(0)}{1 + \xi^2 s^2} \simeq I(0)(1 - \xi^2 s^2) \quad (7)$$

where ξ is Ornstein–Zernike's correlation length. Thus, Debye's correlation length L_D is related to the correlation length ξ by the relation of $L_D = 6^{1/2}\xi$. From the inclination of the scattering curve in the small s region, the gyration radius R_G by Guinier[17] is also obtained. However, in this case, the boundary of the particle gives a clear difference of electron density, while Debye's correlation length can be defined not only for the definite boundary but also for fuzzy boundaries in solution. Therefore, the gyration radius by Guinier is not adopted in the present work. For a system in which Guinier's R_G can be defined, the relation between Debye's correlation length and Guinier's R_G is given by $L_D = 2^{1/2}R_G$. It is noticed that for a sphere with a radius R_0, $L_D = 1.1R_0$; that is, L_D is a measure of radii of the space distribution of the fluctuation of electron density.

Debye's correlation lengths for each temperature determined from the curve fitting of $I(s)$ are shown in Figure 8, in comparison with $6^{1/2}\xi$ obtained by Koga from the SAXS data of TBA–water mixtures at 27 °C.[18] In a comparison of Koga's data (27 °C) and ours at 28 °C, it is seen that both are in qualitative agreement, but not quantitatively.

By the use of the mutual diffusion constant D_m obtained by dynamic light scattering with photon correlation spectroscopy (PCS),[4] Euliss and Sorensen[5] and Bender and Pecora[6] independently reported the correlation length ξ of the TBA–water mixtures. The two results[5,6] are consistent, and the magnitude of the correlation length varies from about 4 to 8 Å in the concentration range $c_1 = 0.073$–0.26 and the temperature range 10–45 °C. Their results are shown in Figure 9, compared with the present results, where the correlation length ξ by PCS are interpreted as the Ornstein–Zernike correlation length according to the interference given in ref 5 and 6. Figure 9 shows that L_D by SAXS and $6^{1/2}\xi$ by PCS are roughly consistent with each other over the measured temperature and concentration ranges and that the size of the space distribution of the fluctuation of electron density represented by L_D by SAXS is nearly the same as that of the moving units measured by PCS.

Mixing State of the Solution. A schematic model for the mixing state of TBA–water mixtures is speculated as follows from the experimental results mentioned above and useful information in literature. This model for the mixing state of TBA–water mixtures is nearly the same as the model by Iwasaki and Fujiyama, constructed by means of thermodynamic calculation of the concentration fluctuation on the basis of the "ideal associated model",[2,3] and well depicted in Figures 8 and 9 of ref 2.

At room temperature and at low concentrations near $c_1 = 0.04$, $TBA(H_2O)_n$ may be a unit whose structure is like that shown in Figure 5 in ref 19 and the unit may move independently. The number n is about 24–28. This model is consistent with the fact that the concentration fluctuation in this concentration range at room temperature is nearly equal to zero and the scattering curve of $c_1 = 0.04$ is almost flat (Figure 3 in ref 1 and Figure 1a). As the concentration of TBA increases, the intensity curves incline, which shows that the $TBA(H_2O)_n$ aggregates form a larger cluster such as $(TBA)_m(H_2O)_l$. The aggregates grow to the utmost in the concentration range of $c_1 \simeq 0.20$. The value of $\rho_\alpha G_{\alpha\beta}$ indicates that both TBA and water have a tendency to gather the same species and to separate from the other component. However, from the comparison of the radial distribution function of pure TBA[20] and that of the TBA–water mixtures of $c_1 = 0.17$,[21] it cannot be

(15) Debye, P. *J. Chem. Phys.* **1959**, *31*, 680.
(16) Ziman, J. M. *Models of Disorder*; Cambridge University Press: Cambridge, 1979.
(17) Guinier, A.; Fournet, G. *Small-Angle Scattering of X-rays*; Wiley: New York, 1955.
(18) Koga, Y. *Chem. Phys. Lett.* **1984**, *111*, 176.
(19) Tanaka, H.; Nakanishi, K.; Nishikawa, K. *J. Inclusion Phenom.* **1984**, *2*, 119.
(20) Narten, A. H.; Sandler, I. *J. Chem. Phys.* **1979**, *71*, 2069.

TABLE II: Number m Estimated from Debye's Correlation Length L_D

	R/Å	
L_D/Å	6	5
7.5	1.0	1.7
10	2.4	4.1
12.5	4.6	8.0
15	8.0	14
17.5	13	22
20	19	33

concluded that TBA (or water) molecules make domains of only one species. In the region of concentrations higher than 0.04, the number of water molecules is not sufficient to surround all the TBA molecules. Therefore, there may exist $(TBA)_m(H_2O)_l$ domains and free TBA regions. It is interpreted that the difference of the electron density between the aggregate, $(TBA)_m(H_2O)_l$, and bulk TBA causes the inclination of the scattering curve and the radius of the aggregate is the same order of magnitude as Debye's correlation length L_D. At concentrations higher than $c_1 \simeq 0.2$, the breakdown of the aggregates may occur, which is suggested by the decrease of the concentration fluctuation and the temperature dependence of the enthalpy change observed for TBA–water mixtures.[22] The model by Iwasaki and Fujiyama[3] is constructed for the rapid increase of the concentration fluctuation at the concentration range larger than $c_1 = 0.05$, and their data are available in the range $0 < c_1 < 0.16$. The decrease of the concentration fluctuation and the decrease of the correlation length at concentrations higher than $c_1 = 0.2$ are not predicted since the breakdown of the aggregates is not assumed in their model calculation.

As the temperature is raised, a portion of the independent unit of $TBA(H_2O)_n$ forms aggregates even at the concentration of $c_1 \simeq 0.04$, which is seen by the fact that the concentration fluctuation becomes slightly larger than zero (Figure 3) and the intensity curves incline (Figure 1b,c). As the concentration increases, the aggregation may proceed and the radius of the clusters become largest at $c_1 \simeq 0.14$–0.17. The higher the temperature is, the bigger the clusters are. However, the hydrogen bonds of water forming the clathrate cage may break down partially in order to decrease the Gibbs' free energy of the system by the effect of the entropy term. The size of the aggregate is about 40 Å ($2L_D$) at 55 °C. In concentrations higher than $c_1 \simeq 0.17$, the aggregates may breakdown and this decomposition may proceed more rapidly than at room temperature because of the effect of the entropy term, judging from the intersecting of the curves of the concentration fluctuation (Figure 3).

The number m of TBA molecules in the aggregate $(TBA)_m(H_2O)_l$ is roughly estimated from Debye's correlation length L_D with the following assumptions: (i) The aggregate is spherical. (ii) The radius of the aggregate is given by $L_D/1.1$. (iii) A TBA molecule is in the form of a clathrate cage shown in Figure 5 in ref 19. (iv) The radius R of the cage is estimated to be ~6 Å when the unit are gathered without face-sharing, and to be ~5 Å when polygons of the clathrate hydrate are face-shared as in the crystal structure of the type II.[23] (v) The packing occupancy is assumed to be 0.7 (the occupancy of the spheres is as follows: simple cubic, 0.52; bcc, 0.68; fcc, 0.74; and crystals of clathrate hydrate of type II, 0.71). Thus, m is calculated by

$$m \simeq \frac{(L_D/1.1)^3}{R^3}0.7 \qquad (8)$$

The result is tabulated in Table II. For example, at 55 °C, the value of $m = 2$–4 at $c_1 = 0.04$, the aggregation proceeds rapidly with the increase of the concentration, and at $c_1 = 0.14$, the number of m reaches 19–33. Then, the breakdown of the aggregate occurs, and the value of m decreases to 5–8 at $c_1 = 0.3$. Iwasaki and Fujiyama estimated the number of m from their ideal associated model as 4–8 at 17.5 °C and 12–22 at 63 °C for the concentration range $c_1 > 0.05$.[3] These values are roughly consistent with the value estimated from Debye's correlation lengths in concentration ranges lower than $c_1 = 0.2$.

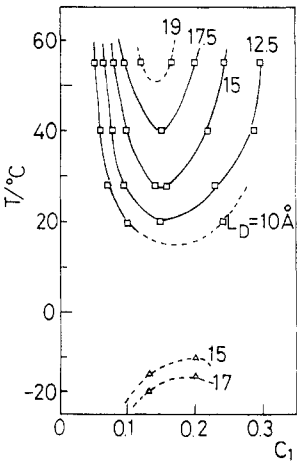

Figure 10. Contour map of the magnitude of Debye's correlation length L_D on the T vs c_1 plane: (□) present results and (△) results from ref 5.

TBA mixes with water at any concentration and at any temperature of the liquid state. However, in the microscopic scale, we may say that TBA molecules are not miscible with water. The order of the discrepancy from the random mixing can be expressed by the concentration fluctuation or the Kirkwood–Buff parameters or the magnitude of the correlation length. We may conceive that L_D is a kind of scale to express the order of magnitude of microscopic demixing or an indication of approaching a critical point or region and that the phase separation occurs when the magnitude of the correlation length reaches a macroscopic scale. Then, we can draw a contour map of the magnitudes of Debye's correlation length L_D on the T vs c_1 plane. The map is shown in Figure 10. Since the SAXS experimental results are limited to the data at room temperature and a few higher temperatures, the results of the supercooled phase by Euliss and Sorensen[5] are also included. From Figure 10, one may say that the TBA–water mixture is a system exhibiting a behavior like multiple phase separation, namely, a closed-loop region in the higher temperature and dome-shaped region in the lower temperature. The possibility of such phase separation was theoretically predicted by Goldstein and Walker,[24] though the present case is regarded not as macroscopic phase separation but as microscopic demixing.

Several authors discussed the existence of the critical demixing of quasi-critical phase separation for TBA–water solution. For example, it is known that the addition of a small amount of an electrolyte such as KCl or NH_4Cl to the solution will cause the appearance of a closed-loop two-phase region in the phase diagram.[5,25,26] Iwasaki and Fujiyama asserted the existence of a pseudo-lower critical solution temperature above the boiling temperature from the behavior of the concentration fluctuation.[2,3] Euliss and Sorensen also suggested the existence of the lower critical solution temperature above the equilibrium boiling point from the correlation length (ξ) obtained from a PCS experiment, and they also discovered anomalous critical-phenomena-type properties in the supercooled mixtures.[5] Bender and Pecora said that no direct evidence was found to verify or disprove the existence of a critical region in the phase space of the mixtures from the results of both the dynamic light scattering experiment and the measurements of hypersonic speed of sound.[6] However, they concluded that the behavior of the system is compatible with a

(21) Nishikawa, K.; Kodera, Y.; Iijima, T., unpublished result. The radial distribution function is shown in Figure 10 in ref 1.
(22) Morcom, K. W.; Smith, R. W. *Trans. Faraday Soc.* **1970**, *66*, 1073.
(23) Mak, T. C. W.; McMullan, R. K. *J. Chem. Phys.* **1965**, *42*, 2732.
(24) Goldstein, R. E.; Walker, J. S. *J. Chem. Phys.* **1983**, *78*, 1492.
(25) Timmermans, J.; Poppe, G. *C. R. Hebd. Sceances Acad. Sci.* **1935**, *201*, 608.
(26) Kato, K.; Yudasaka, M.; Fujiyama, T. *Bull. Chem. Soc. Jpn.* **1982**, *55*, 1284.

model of structural relaxation due to some cooperative motion of a collection of molecules. Neither were they able to discount the existence of short-lived aggregates that have a low optical anisotropy.

Uedaira et al. reported that "long-lived" aggregates do not exist in the TBA–water mixtures since the self-diffusion constants of each component, TBA and water, are different[27] by an NMR study of the spin-echo pulsed-gradient method. This is in apparent contradiction to the description of the mixing state in terms of clusterlike aggregates or a collection of molecules. The discrepancy may be due to the difference of the time scale in these different experimental methods. In the NMR study, the time scale for the long-lived aggregates was longer than 10^{-11} s.[27] In PCS, the relaxation time is on the order of 10^{-3}–10^{-4} s. In the X-ray scattering experiment, the information is an ensemble average over a long time produced by overlapping many instantaneous ($\sim 10^{-17}$ s) arrangements of molecules. X-rays see short-lived aggregates for a long time. It is probable that molecules are quickly ($\sim 10^{-12}$ s) replacing the positions of each other and yet forming aggregates that can be viewed as an ensemble average in X-ray scattering and also detected as a moving unit in light scattering.

Debye's correlation length L_D by small-angle X-ray scattering experiments corresponds to the space distribution of the fluctuation of the electron density. Therefore, the units with the correlation length L_D do not necessarily move together. Comparison in Figure 9 showed that L_D from SAXS cannot be distinguished from the size of the moving units obtained from PCS.

On the basis of an analysis of the mutual diffusion constant of TBA–water mixtures, Ito et al. discussed the moving unit that is defined as a group of molecules that move together for a time much longer than the velocity-correlation time (10^{-13}–10^{-12} s).[28] They concluded that the unit of $TBA(H_2O)_n$ is the moving unit (n is ~ 11 at 24 °C and 19–21 at 63 °C) in the concentration range $0 < c_1 < 0.1$ though the static configuration of the local structure is much larger.[3] The estimated size of such static configuration is consistent with the L_D values of the present study as is discussed in the previous section, while the size of the moving unit is smaller by a factor of 2–3, corresponding to the magnitude of the correlation length ξ by the PCS experiments. In the comparison of Figure 9, both sizes are nearly the same. This discrepancy raises two questions. (1) What is the true physical meaning of ξ determined by the PCS experiment? Is it the Ornstein–Zernike correlation length? (2) To what extent are the results of the complicated analysis of the mutual diffusion constant by Ito et al. robust? Answering these questions is beyond the scope of the present paper and shall be left to future investigations.

Registry No. H_2O, 7732-18-5; *t*-BuOH, 75-65-0.

(27) Uedaira, H.; Kida, J. *Nippon Kagaku Kaishi* **1982**, *4*, 539 (in Japanese).

(28) Ito, N.; Kato, T.; Fujiyama, T. *Bull. Chem. Soc. Jpn.* **1981**, *54*, 2573.

Factors Contributing to Distortion Energies of Bent Hydrogen Bonds. Implications for Proton-Transfer Potentials

Slawomir M. Cybulski and Steve Scheiner*

Department of Chemistry and Biochemistry, Southern Illinois Univerisity, Carbondale, Illinois 62901-4409
(Received: January 19, 1989)

The ab initio interaction energy for the optimal arrangement of a number of H-bonded systems is decomposed and compared to a variety of geometries in which angular deformations are imposed. For cationic systems $(H_3NH\cdots NH_3)^+$ and $(H_2OH\cdots OH_2)^+$, the $(HOH\cdots OH)^-$ anion, and the neutral dimer $(HOH\cdots OH_2)$, the electrostatic term is the largest of the various components and provides a reasonable first approximation to the total interaction energy as a result of mutual cancellation between the remaining terms. Even though the multipole expansion of the electrostatic interaction is not rapidly convergent, its cumulative sum through R^{-5} offers a good approximation to the full electrostatic expression. Most of the distortion energy resulting from angular deformation of the H bond in $(HOH\cdots OH)^-$ is concentrated in the dipole–ion term. The same is true of the cationic systems except that the ion–quadrupole term is of comparable magnitude and should be considered as well. In all these cases, a simple picture based on the preceding interactions is usually capable of predicting the sense of the asymmetry introduced into the proton-transfer potential by a given angular distortion.

I. Introduction

While there have been a good many ab initio calculations of proton-transfer reactions in the past,[1-9] most have considered optimal geometries and have ignored the implications of "bending" of the H bond upon the process. A series of recent calculations of a number of systems[10-16] have indicated that the sense of asymmetry of the proton-transfer potential is intimately connected with angular features of the H bond. Taking the $(H_3N\cdots H\cdots NH_3)^+$ system as an example, the proton-transfer potential is of course completely symmetric when the H bond adopts its most

(1) Liang, J.-Y.; Lipscomb, W. N. *Biochemistry* **1987**, *26*, 5293.
(2) Hiraoka, K.; Mizuse, S.; Yamabe, S.; Nakatsuji, Y. *Chem. Phys. Lett.* **1988**, *148*, 497.
(3) McKee, M. L. *J. Am. Chem. Soc.* **1987**, *109*, 559.
(4) Brciz, A.; Karpfen, A.; Lischka, H.; Schuster, P. *Chem. Phys.* **1984**, *89*, 337.
(5) Ikuta, S.; Nomura, O. *J. Mol. Struct. THEOCHEM* **1987**, *152*, 315.
(6) Osman, R.; Topiol, S.; Rubenstein, L.; Weinstein, H. *Mol. Pharmacol.* **1987**, *32*, 699. Dijkman, J. P.; Osman, R.; Weinstein, H. *Int. J. Quantum Chem., Quantum Biol. Symp.* **1987**, *No. 14*, 211.
(7) Cao, H. Z.; Allavena, M.; Tapia, O.; Evleth, E. M. *J. Phys. Chem.* **1985**, *89*, 1581; *Chem. Phys. Lett.* **1983**, *96*, 458.
(8) Alagona, G.; Desmeules, P.; Ghio, C.; Kollman, P. A. *J. Am. Chem. Soc.* **1984**, *106*, 3623.
(9) Jones, W. H.; Mezey, P. G.; Csizmadia, I. G. *J. Mol. Struct.: THEOCHEM* **1985**, *121*, 85.
(10) Scheiner, S. *Acc. Chem. Res.* **1985**, *18*, 174. Scheiner, S.; Redfern, P.; Hillenbrand, E. A. *Int. J. Quantum Chem.* **1986**, *29*, 817. Scheiner, S. *J. Mol. Struct.* **1988**, *177*, 79.
(11) Scheiner, S. *J. Am. Chem. Soc.* **1981**, *103*, 315; *J. Phys. Chem.* **1982**, *86*, 376; *J. Chem. Phys.* **1982**, *77*, 4039.
(12) Hillenbrand, E. A.; Scheiner, S. *J. Am. Chem. Soc.* **1984**, *106*, 6266.
(13) Scheiner, S.; Hillenbrand, E. A. *J. Phys. Chem.* **1985**, *89*, 3053.
(14) Hillenbrand, E. A.; Scheiner, S. *J. Am. Chem. Soc.* **1985**, *107*, 7690.
(15) Hillenbrand, E. A.; Scheiner, S. *J. Am. Chem. Soc.* **1986**, *108*, 7178–7186.
(16) Cybulski, S. M.; Scheiner, S. *J. Am. Chem. Soc.* **1989**, *111*, 23.

0022-3654/89/2093-6565$01.50/0